# Density functional theory for the phase diagram of rigid $C_{60}$ molecules

M. Hasegawa [1] and K. Ohno [2]
[1]*Department of Materials Science and Technology, Faculty of Engineering, Iwate University, Morioka 020, Japan*
[2]*Institute for Materials Research, Tohoku University, Sendai 980-77, Japan*
(Received 4 April 1996)

A density functional theory of freezing combined with a thermodynamically consistent integral equation method is used to predict the phase diagram of rigid $C_{60}$ molecules interacting via the Girifalco potential. It is found that the freezing line crosses the liquid-vapor binodal lines near the critical point and the liquid phase exists in a very narrow range of temperatures (<20 K), in qualitative agreement with the molecular dynamics (MD) simulations of Cheng *et al.* But, quantitatively, the present result falls between the MD simulations and the Monte Carlo simulations of Hagen *et al.*, the latter of which have predicted nonexistence of a liquid phase. [S1063-651X(96)00110-9]

PACS number(s): 64.70.Dv, 64.30.+t, 64.70.Fx

Since the discovery of fullerenes [1] most studies have focused on the isolated molecules and the solid phases at low temperatures. Recently, the phase behavior of $C_{60}$ at high temperatures has also stimulated increasing interest [2–4]. One of the issues raised by the recent simulation studies is whether $C_{60}$ has a liquid phase as the thermodynamically stable phase. Using the same intermolecular potential proposed by Girifalco [5], Hagen *et al.* have performed Monte Carlo (MC) simulations and concluded that $C_{60}$ has no liquid phase [3], whereas the molecular dynamics (MD) simulations of Cheng *et al.* have predicted the existence of a liquid in a narrow range of temperatures [4]. The Girifalco potential used in these simulations was constructed by assuming that the carbon atoms on different $C_{60}$ molecules interact through a Lennard-Jones (LJ) potential and by averaging the intermolecular potential over all relative orientations of the two $C_{60}$ molecules. The pair potential between $C_{60}$ molecules obtained in this way significantly differs from the LJ form in that its attractive part decays more rapidly than that of the LJ form as the intermolecular separation becomes large [5]. The effects of short-rangedness of intermolecular potentials on the phase behavior and the solid-to-solid transition have been investigated for some model systems with varying ranges of attractive forces [6–15]. Some of these studies have shown that the liquid-vapor coexisting region is immersed in the solid-fluid coexisting region and a liquid phase exists no more as the attractive part of pair potentials becomes sufficiently short ranged [6–10]. The simulation studies on $C_{60}$ suggest that $C_{60}$ is a substance near the border separating existence and nonexistence of a liquid phase [3,4], but its phase behavior is still inconclusive.

In the present contribution we report our theoretical calculations for the phase diagram of $C_{60}$ based on the same Girifalco potential. We use a density functional theory (DFT) of freezing combined with a thermodynamically consistent integral equation method. Since the pioneering work of Ramakrishnan and Yussouff [16], the DFT of freezing has been recognized as a powerful tool in the study of solid-fluid phase transitions [17]. In the present study we have used a generalized version of the modified weighted-density approximation (MWDA) developed by Denton and Ashcroft [18]. This generalized MWDA (GMWDA) is based on the idea of the thermodynamic perturbation theory developed for uniform liquids [19] and has been applied to predict the solid-liquid phase transition of the classical one-component plasma (OCP) and the inverse-power systems [20]. The GMWDA is summarized in the following.

We consider a system interacting through a pair potential $\phi(r)$, and start with splitting $\phi(r)$ into two parts, $\phi(r)=\phi_0(r)+\Delta\phi(r)$, where $\phi_0(r)$ is a repulsive, short-ranged part and $\Delta\phi(r)$ is the remaining long-ranged part. The free energy of the system as a functional of (number) density $\rho(\mathbf{r})$ is then written, in accordance with this splitting, as

$$F[\rho]=F_{\mathrm{id}}[\rho]+F_{0,\,\mathrm{ex}}[\rho]+F_1[\rho], \tag{1}$$

where $F_{\mathrm{id}}[\rho]$ is the ideal-gas contribution, $F_{0,\mathrm{ex}}[\rho]$ the excess free energy of the *reference* system interacting through $\phi_0(r)$, and $F_1[\rho]$ the contribution due to $\Delta\phi(r)$. The functional form of $F_{\mathrm{id}}[\rho]$ is known as [17]

$$F_{\mathrm{id}}[\rho]=\beta^{-1}\int d\mathbf{r}\rho(\mathbf{r})\{\ln[\rho(\mathbf{r})\Lambda^3]-1\}, \tag{2}$$

where $\beta=1/k_BT$ and $\Lambda$ is the thermal de Broglie wavelength. Various versions have been developed based on this approach and major differences between them consist in the choice of the reference system and in the treatment of $F_1[\rho]$ [20–23]. For an appropriate potential separation the reference free energy $F_{0,\mathrm{ex}}[\rho]$ is mostly entropic and the contribution $F_1[\rho]$ accounts for most of the excess internal energy. Curtin and Ashcroft noted the importance of treating these contributions to the free energy by separate approximations [21]. Following the MWDA and others [17], we make separate global thermodynamic mappings for $F_{0,\mathrm{ex}}[\rho]$ and $F_1[\rho]$:

$$F_{0,\mathrm{ex}}[\rho]\approx Nf_{0,\mathrm{ex}}(\hat{\rho}_0) \tag{3a}$$

and

$$F_1[\rho]\approx Nf_1(\hat{\rho}_1), \tag{3b}$$

 

where $N$ is the number of particles in the system, $f_{0,\mathrm{ex}}(\rho)$ the excess free energy per particle of a homogeneous reference fluid, and $f_1(\rho)=f_{\mathrm{ex}}(\rho)-f_{0,\mathrm{ex}}(\rho)$, $f_{\mathrm{ex}}(\rho)$ being the total excess free energy of the system. We assume that the effective-liquid densitites, $\hat{\rho}_0$ and $\hat{\rho}_1$, are given, as in the MWDA, by

$$\hat{\rho}_0=\frac{1}{N}\int d\mathbf{r}_1\int d\mathbf{r}_2\rho(\mathbf{r}_1)\rho(\mathbf{r}_2)w_0(r_{12};\hat{\rho}_0) \tag{4a}$$

and

$$\hat{\rho}_1=\frac{1}{N}\int d\mathbf{r}_1\int d\mathbf{r}_2\rho(\mathbf{r}_1)\rho(\mathbf{r}_2)w_1(r_{12};\hat{\rho}_1), \tag{4b}$$

where $r_{12}=|\mathbf{r}_1-\mathbf{r}_2|$. The weight functions $w_0$ and $w_1$, as yet unspecified, are determined in the same way as that of the original MWDA [18]. More specifically, we require that both $w_0$ and $w_1$ be normalized and that approximate $F_{0,\mathrm{ex}}[\rho]$ and $F_1[\rho]$ in Eq. (3) exactly reproduce the corresponding two-body direct correlation functions (DCF's), $C_0^{(2)}(r;\rho)$ and $\Delta C^{(2)}(r;\rho)=C^{(2)}(r;\rho)-C_0^{(2)}(r;\rho)$, in the limit of a uniform density. Here $C_0^{(2)}$ and $C^{(2)}$ are the DCF's of the reference and full systems, respectively. Unique specifications of the weight functions follow from these requirements and the substitutions of these results into Eqs. (4a) and (4b) lead to the implicit equations for $\hat{\rho}_0$ and $\hat{\rho}_1$ [20],

$$(\hat{\rho}_0-\overline{\rho})\beta f'_{0,\mathrm{ex}}(\hat{\rho}_0)=-\frac{1}{2N}\int d\mathbf{r}_1\int d\mathbf{r}_2\Delta\rho(\mathbf{r}_1)\Delta\rho(\mathbf{r}_2)\times C_0^{(2)}(r_{12};\hat{\rho}_0) \tag{5a}$$

and

$$(\hat{\rho}_1-\overline{\rho})\beta f'_1(\hat{\rho}_1)=-\frac{1}{2N}\int d\mathbf{r}_1\int d\mathbf{r}_2\Delta\rho(\mathbf{r}_1)\Delta\rho(\mathbf{r}_2)\times\Delta C^{(2)}(r_{12};\hat{\rho}_1), \tag{5b}$$

where $f'_{0,\mathrm{ex}}(\rho)=\partial f_{0,\mathrm{ex}}(\rho)/\partial\rho$, $f'_1(\rho)=\partial f_1(\rho)/\partial\rho$, and $\Delta\rho(\mathbf{r})=\rho(\mathbf{r})-\overline{\rho}$, $\overline{\rho}$ being the average density of the solid under consideration. We note that both $\hat{\rho}_0$ and $\hat{\rho}_1$ are functionals of $\rho(\mathbf{r})$ and are determined by solving Eqs. (5a) and (5b), respectively, for a given $\rho(\mathbf{r})$. The approximate excess free energy per particle of the solid phase is then given by

$$\beta f_{\mathrm{ex}}[\rho]\approx\beta f_{0,\mathrm{ex}}(\hat{\rho}_0)+\beta f_1(\hat{\rho}_1). \tag{6}$$

We have applied the above theory to the inverse-power systems with $\phi(r)=\varepsilon(\sigma/r)^n$ and found that the theory predicts the fcc-solid-liquid phase boundaries in agreement with the MC results within 5%, although it does not necessarily predict the correct equilibrium crystal structure (i.e., bcc for $n<7$ and fcc for $n>7$) of the solid coexisting with the liquid [20]. We have also confirmed that $\hat{\rho}_0\lesssim\overline{\rho}$ and $\hat{\rho}_1\approx\overline{\rho}$ for a stabilized solid in the variational calculations described below. The large difference between $\hat{\rho}_0$ and $\hat{\rho}_1$ provides a simple, intuitive explanation for the reason why the MWDA and other theories utilizing the thermodynamic mapping on a single effective liquid fail for systems with long-ranged or attractive forces. As noted above, the contribution $F_{0,\mathrm{ex}}[\rho]$ is mostly entropic and the large difference between $\hat{\rho}_0$ and $\overline{\rho}$ is a consequence of the fact that the excess entropy of the solid is much smaller (in magnitude) than that of the liquid with the same density. On the other hand, the contribution $F_1[\rho]$ accounting for most of the excess internal energy is not much different in the solid and the liquid phases. Consequently, $\hat{\rho}_1$ and $\overline{\rho}$ should not differ so much from each other, as actually confirmed [20], and the term on the right-hand-side of Eq. (5b) should be small, which is nothing but the situation where the second-order perturbation theory (SPT) is expected to work well for $F_1[\rho]=Nf_1[\rho]$. In this SPT we have

$$\beta f_1[\rho]\approx\beta f_1(\overline{\rho})-\frac{1}{2N}\int d\mathbf{r}_1\int d\mathbf{r}_2\Delta\rho(\mathbf{r}_1)\Delta\rho(\mathbf{r}_2)\Delta C^{(2)}\times(r_{12};\overline{\rho}). \tag{7}$$

Curtin and Ashcroft have used Eq. (7) together with the hard-sphere (HS) reference system and successfully calculated the phase diagram of the LJ system [21].

In the application of the above theory to $C_{60}$ we used the potential separation proposed by Weeks, Chander, and Andersen (WCA) [24].

$$\phi_0(r)=\begin{cases}\phi(r)-\phi(r_0, & r<r_0\\ 0, & r>r_0\end{cases}, \tag{8}$$

where $r_0$ is the separation at which $\phi(r)$ takes the principal minimum. For the Girifalco potential we have $x_0=r_0/2a=1.416\,342$, where $2a$ is the diameter of a spherical $C_{60}$ given by $2a=0.71$ nm [5].

The modified hypernetted-chain (MHNC) theory [25] was used to calculate the equation of state and the DCF's of the systems interacting through $\phi(r)$ and $\phi_0(r)$, which are a necessary input to solve Eqs. (5a) and (5b) and to determine the liquid-vapor phase boundary. Several versions in the context of the MHNC theory have been proposed, and their differences consist in dealing with the hard-sphere bridge function $B_{\mathrm{HS}}(r)$ used in this theory. In his study on the phase diagram of $C_{60}$ molecular fluid [26], Caccamo has used the $B_{\mathrm{HS}}(r)$ obtained from the Verlet-Weis parametrization of the HS radial distribution function [27,28], and imposed the thermodynamic consistency between the virial pressure and the compressibility equations to specify the parameter of $B_{\mathrm{HS}}(r)$. We took essentially the same approach but solved the MHNC equation for the full system with $\phi(r)$ by using the method of Ng [29], which is essential for Coulombic systems and provides an efficient way for other systems with long-ranged potentials. In this method the long-range tail of the DCF due to that of $\phi(r)$, $\Delta\phi(r)$ in the present case, is separated out and we solve the MHNC equation for $C_s(r)=C(r)+\beta\Delta\phi(r)$. In solving the MHNC equation we used a grid spacing $\Delta x=0.025(x=r/2a)$ and a grid of 1024 points with an extra fine grid spacing $\Delta x=0.0025$ in the core region where $\phi(r)$ or $\phi_0(r)$ and hence $C(r)$ exhibit rapid changes.

In the calculations of the free energy of the solid phase in the GMWDA we followed the common practice and used a variational method, in which the density distribution in the solid was parametrized and given by the sum of the Gaussians peaked at each site of a periodic lattice, $[R_i]$:

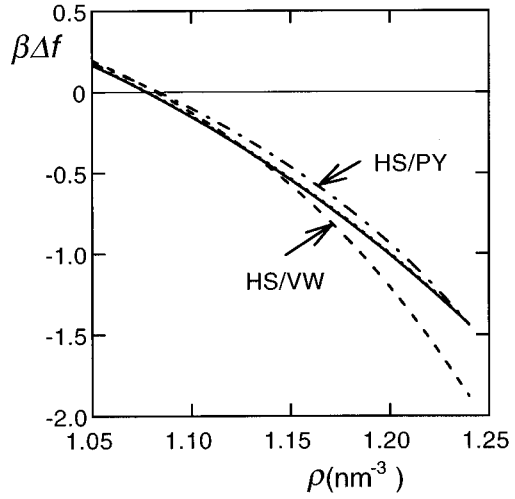


FIG. 1. Comparisons of the free energies of the fcc solid $C_{60}$ relative to the liquid [Eq. (10)] at $T=2100$ K calculated by the present GMWDA with the WCA reference system (8) (full line) and by the method of using the HS reference system with the VW DCF (HS-VW) and the PY DCF (HS-PY). The result obtained using the SPT for $\beta f_1[\rho]$ [Eq. (7)] (dotted line) is almost indistinguishable from the GMWDA result.

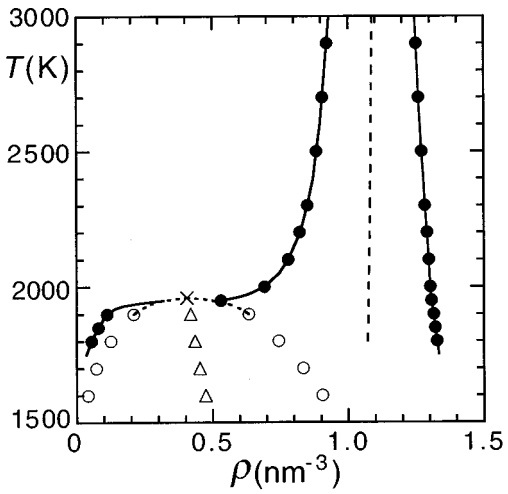


FIG. 2. Phase boundaries predicted by the present theory (filled circles and full lines). Open circles, metastable liquid-vapor binodal lines; triangles, rectilinear rule used to locate the critical point (cross); dashed line, freezing line determined by the one-phase criterion [Eq. (11)].

$$\rho(\mathbf{r})=\left(\frac{\alpha}{\pi}\right)^{3/2}\sum_i \exp[-\alpha(\mathbf{r}-\mathbf{R}_i)^2]. \tag{9}$$

Then, the variational principle for the free energy reduces to a minimization of $F[\rho]=Nf(\rho;\alpha)$ with respect to $\alpha$. We assumed the fcc crystal structure for the $C_{60}$ solid phase.

Figure 1 illustrates the calculated free energies of the solid relative to the liquid with the same density, which plays a crucial role in determining the solid-liquid phase boundary:

$$\beta\Delta f(\rho)=\beta f_{\text{solid}}(\rho)-\beta f_{\text{liq}}(\rho), \tag{10}$$

where $f_{\text{liq}}(\rho)\equiv f(\rho;\alpha=0)$ and $f_{\text{solid}}(\rho)\equiv f(\rho;\alpha)$, with $\alpha$ minimizing $f$. The most popular practice in the approach described above has been to employ the HS reference system [21–23], and Fig. 1 also contains the results of such calculations for comparison. In these calculations the reference HS parameters were determined by applying the method of Andersen and co-workers [19,30] to the WCA reference system (8). The corresponding MWDA equation (5a) was solved by using both the virtually exact Verlet-Weis (VW) [27,28] and the approximate Percus-Yevick (PY) DCF's. Hereafter, these types of calculations are denoted HS-VW and HS-PY, respectively. The use of the PY DCF has been justified based on the observation that for a realistic solid with large $\alpha$ the solution $\hat{\rho}_0$ to Eq. (5a) is much smaller than $\rho$, the average density of the solid under consideration, and for such a $\hat{\rho}_0$ the PY DCF is quite reasonable. In all these calculations the accurate Carnahan-Starling [19] result was used for $f_{0,\text{ex}}(\rho)\equiv f_{\text{HS,ex}}(\rho)$ in (5a) and the contribution $f_1[\rho]$ was calculated by the SPT (7) with the use of the accurate $\Delta C(r;\overline{\rho})$ obtained from the present MHNC result for $C(r;\overline{\rho})$ and the VW result for $C_0(r;\overline{\rho})\equiv C_{\text{HS}}(r;\overline{\rho})$. We find in Fig. 1 that the HS-VW and the HS-PY yield quite different results for $\beta\Delta f(\rho)$, contrary to the previous expectation. Both of these $\beta\Delta f(\rho)$ decrease too rapidly with $\rho$ and yield too large negative contributions to the pressures of the solid at high densities to establish a phase equilibrium of the solid and the liquid. The previous reexaminations of the MWDA and the generalized effective-liquid approximation (GELA) of Lutsko and Baus [31] revealed that the use of an accurate DCF in place of the approximate PY DCF in these theories slightly worsens the predicted HS freezing parameters, which is an unfavorable feature from a theoretical point of view [32]. Furthermore, such a feature becomes much more serious when the HS system is used as the reference system for systems with long-ranged potentials, as actually confirmed for the OCP [32]. Such a situation is common to $C_{60}$, and it seems that the defect of using the HS reference system is compensated by that of the approximate PY DCF, but we need further examinations to clarify the defect of using the HS reference system for $C_{60}$. In the following we consider only the results of the GMWDA based on the WCA reference system (8) and the input data obtained by the thermodynamically consistent integral equation method.

The phase boundary was determined by enforcing equality of pressures and chemical potentials in the two coexisting phases at fixed temperature. The phase diagram of $C_{60}$ calculated in this way is shown in Fig. 2. We find that the freezing line crosses the liquid-vapor binodal lines at $T\approx 1940$ K slightly ($\approx 20$ K) below the estimated liquid-vapor critical temperature $T_c$, and a liquid phase does exist in a very narrow range of temperatures. This result is in qualitative agreement with the MD simulations [4], which have predicted the existence of a liquid phase in a much wider range, i.e., between 1700 and 1950 K. The liquid-vapor coexisting region is determined solely by the equation of state of uniform fluids, and the present and other results [4,29] based on the thermodynamically consistent integral equation methods are quite similar, suggesting that the result of this part is well established. The liquid-vapor coexisting region predicted by the MD simulations is much narrower

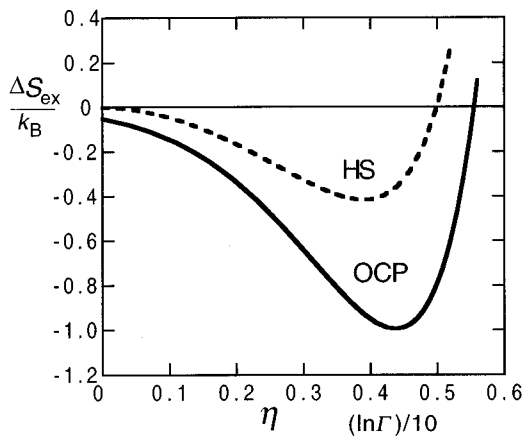


FIG. 3. Multiparticle contribution to the excess entropy of the hard-spheres (HS) and the classical one-component plasma (OCP).

than these theoretical results, and it seems that the MD simulations have detected the boundary of absolute instability, i.e., negative compressibility. The present result for the freezing line falls at somewhat lower densities than the MD result, leading to a narrower range of a liquid phase.

We note that the predicted phase diagram of $C_{60}$ is rather sensitive to the input data within the GMWDA. Prior to the present work we tried the input data obtained by the variational MHNC [33]. The pressure and the compressibility equations of state obtained by this method are different, and the inconsistency is larger at higher densities. While the liquid-vapor critical points estimated by using these input data are almost the same as those in Fig. 2, the predicted freezing lines are quite different. In fact, if we use the input data from the pressure equation, the freezing line passes about 100 K above the critical point, whereas it moves down a great deal, yielding the triple point at $\approx$1800 K, if we use the input data from the compressibility equation. These results suggest the importance of using thermodynamically consistent input data.

Figure 2 also contains the freezing line determined by the one-phase criterion introduced by Giaquinta and Giunta [34],

$$\Delta s_{ex} \equiv s_{ex} - s_{ex}^{(2)} = 0. \quad (11)$$

Here $s_{ex}$ is the exact excess entropy and $s_{ex}^{(2)}$ the two-particle contribution to $s_{ex}$ given by

$$s_{ex}^{(2)} = -\tfrac{1}{2} k_B \rho \int d\mathbf{r}\{g(r)\ln[g(r)] - [g(r)-1]\}, \quad (12)$$

where $g(r)$ is the radial distribution function. The empirical criterion Eq. (11) has been found to give a good prediction of the HS freezing [34] and used by Caccamo in the study of the phase diagram of $C_{60}$ [26]. The present result for the freezing line determined by Eq. (11) is essentially the same as that of Caccamo and falls at much higher densities than the
GMWDA result. It seems that the one-phase criterion (11) overestimates the freezing density of systems with soft-core or long-ranged potentials. Figure 3 illustrates our results of $\Delta s_{ex}$ for the OCP, the extreme case of the long-ranged potential, together with the result for the HS system for comparison. We confirmed that $\Delta s_{ex}=0$ occurs at $\eta=0.499$ for the HS system, in good agreement with the freezing point, $\eta=0.494$, obtained by the MC simulations [35]. On the other hand, the freezing (and melting) point of the OCP determined by Eq. (11) falls at $\Gamma \approx 230$, which is much larger than the MC results, $\Gamma \approx 170$–$180$ [36,37]. Here $\Gamma$ is the usual plasma parameter proportional to $\rho^{1/3}$.

Next, we are concerned with the MC simulation results of Hagen *et al.* [3], which are qualitatively different from the MD and the present results. We note that in the MC simulations the pair potential $\phi(r)$ was truncated at $r=2\sigma$, where $\sigma$ is the distance at which $\phi(r)$ crosses zero, and the predicted $T_C$ was $\approx$1800 K, about 10% lower than the present and the MD simulation results. This low $T_C$ might be a consequence of the truncation of the potential as suggested by the MC simulations for the LJ fluids, in which $T_C$ is about 20% lowered by truncating (and shifting) the LJ potential at $r=2.5\sigma$ [38]. Since the long-range tail of the $C_{60}$ pair potential is much smaller in magnitude than that of the LJ potential, such a truncation effect on $T_C$ should be much smaller in $C_{60}$ but may not necessarily be ignored. In fact, if we shift upwards the MC result of the liquid-vapor coexisting region about 10%, the resulting phase diagram is quite similar to the present result. More quantitative investigations of the truncation effect on the phase diagram of $C_{60}$ are in progress.

Our final concern is the experimental feasibility of testing the theoretical predictions. The estimated liquid-vapor critical pressure is $\approx$32 bar and not so high as to cause any experimental difficulty, but the temperatures of interest ($T>1900$ K) are not easily accessible experimentally. As for the validity of the model of rigid $C_{60}$ molecules, the recent *ab initio* MD simulations have predicted that a $C_{60}$ molecule is stable against fragmentation up to 4500 K [39]. However, polymerizations of $C_{60}$ molecules seem to occur well below the temperatures of interest [40], which could be practically the most serious hindrance to experiments.

We have applied the GMWDA combined with an integral equation method to the calculations of the phase diagram of the rigid $C_{60}$ molecules and found that the results support the existence of a liquid phase, albeit in a very narrow range of temperatures. However, the result is still not very conclusive, since it might depend rather sensitively on the theoretical ingredient, especially on the DFT of freezing used to calculate the equation of state of the solid phase. We may safely conclude that we have confirmed that the rigid $C_{60}$ is a critical substance that might have a liquid phase or not. More systematic investigations will be required to clarify the interrelation between the nature of pair potentials and the phase behavior, and such a theoretical investigation on the systems with $n$-$m$ potentials is in progress as a reinforcement of the simulation studies of Hafskjold [10].

This work has been financially supported by the Grant-in-Aid for Scientific Research on Priority Areas under Grant No. 07236105. Part of this work was carried out under the Visiting Researcher's Program of the Institute for Materials Research (IMR), Tohoku University. We would like to thank the Computer Center at Iwate University and the HITACS-3800/380 Supercomputing System at IMR for providing us with computing facilities.

[1] H. W. Kroto *et al.*, Nature **318**, 162 (1985).
[2] N. W. Ashcroft, Europhys. Lett. **16**, 355 (1991); Nature **365**, 387 (1993).
[3] M. H. J. Hagen *et al.*, Nature **356**, 425 (1993).
[4] A. Cheng *et al.*, Phys. Rev. Lett. **71**, 1200 (1993).
[5] L. A. Girifalco, J. Phys. Chem. **96**, 858 (1992).
[6] M. H. J. Hagen and D. Frenkel, J. Chem. Phys. **101**, 4093 (1994).
[7] L. Mederos and G. Navascués, J. Chem. Phys. **101**, 9841 (1994).
[8] C. F. Tejero *et al.*, Phys. Rev. Lett. **73**, 752 (1994).
[9] T. Coussaert and M. Baus, Phys. Rev. E **52**, 862 (1995).
[10] B. Hafskjold (private communication).
[11] P. Bolhuis and D. Frenkel, Phys. Rev. Lett. **72**, 2211 (1994).
[12] P. Bolhuis *et al.*, Phys. Rev. E **50**, 4880 (1994).
[13] C. N. Likos *et al.*, J. Phys. Condens. Matter **6**, 10 965 (1994).
[14] Zs. T. Németh and C. N. Likos, J. Phys. Condens. Matter **7**, L537 (1995).
[15] C. N. Likos and G. Senatore, J. Phys. Condens. Matter **7**, 6797 (1995).
[16] T. V. Ramakrishnan and M. Yussouff, Phys. Rev. B **19**, 2775 (1979).
[17] See, for example, R. Evans, in *Fundamentals of Inhomogeneous Fluids*, edited by D. Henderson (Dekker, New York, 1992), p. 85.
[18] A. R. Denton and N. W. Ashcroft, Phys. Rev. A **39**, 4701 (1989).
[19] J.-P. Hansen and I. R. McDonald, *Theory of Simple Liquids*, 2nd ed. (Academic, London, 1986).
[20] M. Hasegawa, J. Phys. Soc. Jpn. **62**, 4316 (1993); **63**, 2215 (1994).
[21] W. A. Curtin and N. W. Ashcroft. Phys. Rev. Lett. **26**, 2775 (1986).
[22] J. F. Lutsko and M. Baus, J. Phys. Condens. Matter **3**, 6547 (1991).
[23] L. Mederos *et al.*, Phys. Rev. E **47**, 4284 (1993).
[24] J. D. Weeks *et al.*, J. Chem. Phys. **54**, 5237 (1971).
[25] Y. Rosenfeld and N. W. Ashcroft, Phys. Rev. A **20**, 1208 (1979).
[26] C. Caccamo, Phys. Rev. B **51**, 3387 (1995).
[27] L. Verlet and J. J. Weis, Phys. Rev. A **5**, 939 (1972).
[28] D. Henderson and E. W. Grundke, J. Chem. Phys. **63**, 601 (1975).
[29] K. -C. Ng, J. Chem. Phys. **61**, 2680 (1974).
[30] H. C. Andersen *et al.*, Phys. Rev. A **4**, 1597 (1971).
[31] J. F. Lutsko and M. Baus, Phys. Rev. A **41**, 5547 (1990).
[32] M. Hasegawa, J. Phys. Soc. Jpn. **64**, 4242 (1995); **64**, 4248 (1995).
[33] Y. Rosenfeld, Phys. Rev. A **29**, 2877 (1984); J. Stat. Phys. **42**, 437 (1986).
[34] P. V. Giaquinta and G. Giunta, Physica (Amsterdam) **187A**, 145 (1992).
[35] W. G. Hoover and F. M. Ree, J. Chem. Phys. **49**, 3609 (1968).
[36] G. S. Stringfellow *et al.*, Phys. Rev. A **41**, 1105 (1990).
[37] D. H. Dubin, Phys. Rev. A **42**, 4972 (1990).
[38] B. Smit, J. Chem. Phys. **96**, 8639 (1992).
[39] K. Ohno *et al.*, Phys. Rev. B **53**, 4078 (1996).
[40] A. M. Rao *et al.*, Science **259**, 955 (1993).